A symbolic LFT approach for robust flutter analysis of high-order models

Andrea Iannelli[1], Andrés Marcos[1], Rocco Bombardieri[2] and Rauno Cavallaro[2]

***Abstract*— The paper proposes an alternative methodology to build Linear Fractional Transformation (LFT) models of uncertain aeroelastic systems described by Fluid-Structure Interaction (FSI) solvers with the aim of studying flutter with the μ analysis technique from robust control. Two main issues can be identified for the fulfillment of this task. On the one hand, there is the difficult reconciliation between sources of physical uncertainty (well distinguishable in the original high-order system) and the abstracted uncertainties (defined in the reduced-order size representation used for the robust analyses). On the other hand, the large size of the resulting LFT model can prevent the application of robust analysis techniques. The solution proposed here consists of a symbolic LFT algorithm applied at FSI solver level, which guarantees the connection between the physical uncertainties and the parameters captured by the LFT. It also alleviates the final size of the LFT by exploiting the modal-oriented approach taken in introducing the uncertainties. Application of the framework using an unconventional aircraft layout as case study is finally discussed.**

I. Introduction

Aeroelasticity studies the interaction between elastic and aerodynamic forces on a flexible structure. Among the phenomena arising due to this coupling, particulary relevant is flutter, a self-excited dynamic instability which can have serious consequences on the safe operation of the system and thus might impact the whole system design [1]. The common practice in the field is to characterize the onset and mechanisms underlying flutter by means of dedicated fluid-structure interaction (FSI) solvers. They can provide different levels of fidelity in the description of the flutter problem, but are less efficient in coping with the analysis of systems subject to uncertainties. In fact, while they have the advantage of capturing directly the physical uncertainty, the analyses can only be applied to a defined parameter combination, and due to their computational cost, it is typically only possible to consider a few selected cases.

This is an important aspect, since one of the main issues in flutter analysis originates from the sensitivity of this instability to modeling assumptions and to variations in the nominal values of the parameters [2]. For this reason the community has looked into possible strategies to systematically take into account the effect of uncertainties [3]. Among the proposed approaches there is the so-called robust flutter analysis, which aims to quantify the gap between nominal predictions and the worst-case scenario when uncertainties are considered. It builds on techniques from the robust control community, namely Linear Fractional Transformation (LFT) representations and μ analysis [4]. Foundational contributions are those from [5] and [6], which provided an end-to-end process, from robust modeling to analysis, and demonstrated the validity of the approach. Complementing these works, reference [7] considered in more detail the LFT model development path for flutter problems, and investigated the effect of different modeling options, with particular focus on aerodynamics, on the results.

This article takes the cue from [7] and addresses some of the issues arising when the LFT-μ framework is applied to aeroelastic models of generic complexity. The main aim is to propose a modeling approach which allows to obtain LFT models where the uncertainties have a direct connection with the physical parameters defined in the high-fidelity FSI solver. It is noted that the reconciliation between physical sources of uncertainty in the FSI model and the uncertain parameters in the LFT model is a paramount aspect for an efficient application of μ analysis, and yet this has not received full consideration by the aeronautic community. For example, in [5], [6] the uncertainties in the structural operators consisted of modal quantities (e.g. natural frequencies), whereas [8], [9] considered physical sources of uncertainties but the examples were restricted to a small number, and specific types, of parameters.

The layout of the paper is as follows. Sec. II provides the essential theoretical background, while Sec. III presents the main contribution of the work. This consists of a symbolic LFT approach aimed at tackling the aforementioned issues by performing the required LFT modeling steps embedded in the FSI solver. The effectiveness of the approach is demonstrated in Sec. IV on a joined-wing aircraft of the Prandtlplane type [10], [11], which is known to exhibit a complex aeroelastic behaviour and hence would highly benefit from tools which allow a better understanding of the aeroelastic properties.

II. Background

This section presents a cursory overview of the main tools used in the work. The interested reader is referred to [4] for the robust control and [1] for the fluid-structure interaction parts.

*This work was partially funded by the European Union's Horizon 2020 research and innovation programme under grant agreement No 636307, project FLEXOP.

[1] Andrea Iannelli and Andrés Marcos are with the Department of Aerospace Engineering, University of Bristol, UK andrea.iannelli/andres.marcos@bristol.ac.uk

[2] Rocco Bombardieri and Rauno Cavallaro are with the Department of Bioengineering and Aerospace Engineering, Universidad Carlos III de Madrid, Spain rocco.bombardieri/rauno.cavallaro@uc3m.es

A. Robust control techniques: LFT and μ

The LFT paradigm provides a framework for analysis of uncertain systems by representing them as a feedback interconnection between a known (linear) and an unknown (uncertain) part. Let M be a complex matrix partitioned as $M = [M_{11}\ M_{12};\ M_{21}\ M_{22}]$ and Δ a generic uncertainty set. A particular instance, relevant to the work presented here, is the structured uncertainty set gathering parametric and dynamic uncertainties:

$$\begin{aligned} &\Delta = \text{diag}(\delta_i I_{d_i}, \delta_j I_{d_j}, \Delta_{D_k}) \\ &i = 1, ..., n_R;\ \ j = 1, ..., n_C;\ \ k = 1, ..., n_D; \end{aligned} \tag{1}$$

where the uncertainties associated to n_R real scalars, n_C complex scalars, and n_D full complex blocks are listed in diagonal format (and where I denotes the identity matrix of dimension equal to the number of repetitions of the corresponding parameter).

The upper LFT with respect to Δ can be defined as:

$$\mathcal{F}_u(M, \Delta) = M_{22} + M_{21}\Delta(I - M_{11}\Delta)^{-1}M_{12} \tag{2}$$

A crucial feature apparent in (2) is that the LFT is well posed if and only if the inverse of $(I - M_{11}\Delta)$ exists. Otherwise, $\mathcal{F}_u(M, \Delta)$ is said to be singular. Typically Δ is normalized by scaling of M such that $\mathcal{F}_u(M, 0)$ coincides with the nominal system (i.e. uncertain parameters at their nominal values) and the bound $\bar{\sigma}(\Delta) \leq 1$ holds for uncertainties taking values in the allowed interval. The process of building up LFT models can be efficiently performed by means of available toolboxes (as the LFR toolbox [12] employed here) which directly provide the partitioned matrix M for a given set Δ.

Given the LFT representation of an uncertain linear system, the μ analysis technique allows to quantify robustness in the face of structured uncertainties. The definition follows:

$$\mu_\Delta(M) = \frac{1}{\min\limits_{\Delta}\{\kappa : \det(I - \kappa M\Delta) = 0;\ \bar{\sigma}(\Delta) \leq 1\}} \tag{3}$$

and $\mu_\Delta(M) = 0$ if the minimization problem has no solution. The result of the robust stability (RS) test can then be interpreted as follows: if $\mu_\Delta(M) \leq 1$ then there is no perturbation matrix inside the allowable set Δ such that the determinant condition is satisfied, that is, $\mathcal{F}_u(M, \Delta)$ is well posed and thus the associated plant is robust stable within the range of uncertainties considered. On the contrary, if $\mu_\Delta(M) \geq 1$ a candidate (i.e. belonging to the allowed set) perturbation matrix exists that violates the well-posedness of the LFT, i.e. the underlying uncertain system is not robust stable.

It is known that $\mu_\Delta(M)$ is in general an NP-hard problem, thus all μ algorithms work by searching for upper μ_{UB} and lower μ_{LB} bounds, with the latter also providing the associated matrix Δ^{cr} satisfying the determinant condition. All the results presented in this work use the algorithms as implemented in the Robust Control Toolbox (RCT) in MATLAB R2015b [13].

B. FSI solver

A general expression for the equation governing the interaction between elastic and aerodynamic forces can be written in frequency-domain as:

$$\left[-\omega^2 \bar{M}_s + i\omega \bar{C}_s + \bar{K}_s - q_\infty Q_{hh}(i\omega)\right]\eta = 0 \tag{4}$$

where $q_\infty = \frac{1}{2}\rho_\infty V^2$ is the dynamic pressure, ρ_∞ is the air density, V is the speed, ω the frequency, $\bar{M}_s$, $\bar{C}_s$, $\bar{K}_s \in \mathbb{R}^{n_s \times n_s}$ represent respectively the generalized structural mass, damping and stiffness matrices, Q_{hh} is the generalized aerodynamic force (GAF) coefficient matrix, and η the generalized coordinates vector. The system exhibits self-sustained oscillations when Eq. (4) has a solution for non-trivial η, and generally the main objective in flutter analysis is the determination of the smallest speed such that this occurs, i.e. the flutter speed V_f.

The generalized structural matrices are obtained with modal truncation from their *physical* counterparts M_s, C_s, $K_s \in \mathbb{R}^{N_s \times N_s}$, with N_s indicating the number of structural degrees of freedom, as:

$$\begin{aligned} \bar{M}_s &= \Phi^T M_s \Phi \\ \bar{C}_s &= \Phi^T C_s \Phi \\ \bar{K}_s &= \Phi^T K_s \Phi \end{aligned} \tag{5}$$

where $\Phi \in \mathbb{R}^{N_s \times n_s}$ is the matrix of n_s normal modes. This matrix is obtained from the solution of the classic eigenvalue-eigenvector free vibration problem and, thus, depends on M_s and K_s. For flutter analysis purposes, it typically holds $n_s \ll N_s$ [1]. The FSI solver adopted in this work, named CSHELL and developed by the authors of references [14], [15], provide the operators in (4)-(5). Specifically, the computational solid dynamics module relies on the Finite Element (FE) approach, while for the aerodynamic one the Doublet Lattice Method (DLM) [16] is used. A brief overview of the main features is provided next.

The FE solver is based on beam elements modelled according to Euler-Bernoulli theory [17]. The mass and stiffness matrices are first constructed at element's level, where the various contributors are added (e.g. bending and axial terms for the stiffness matrix). Note that at this stage the operators are a function of physical quantities (e.g. moments of inertia, masses, thicknesses). Then, the (global) FE operators are built up through the well-known procedure of *matrix assembly* [17]. Damping is typically modelled directly in terms of the generalized matrix $\bar{C}_s$, which can be easily obtained for example from the damping ratios associated with each structural mode and the corresponding natural frequencies.

As for the aerodynamic operator, the DLM solver provides, at a fixed reduced frequency $k = \frac{\omega L_r}{V}$ (with L_r reference length), the transfer matrix Q_{hh} from generalized displacements to generalized aerodynamic forces. The fundament for its derivation is the singular integral equation derived from lifting surface theory for harmonic motion [14]. The numerical solution provides the generic coefficient of the GAF matrix $Q_{hh,ij}$, representing the aerodynamic

force generated by the structural mode j and projected onto mode i. It is important to remark that, since the GAF represents a transfer matrix between generalized quantities, its computation depends on the structural modes Φ (which are provided as input to the DLM code).

LFT models of uncertain aeroelastic systems can be derived starting from the description provided in the frequency-domain (4) or in state-space, as detailed in [7] where features of both approaches were studied. The latter one was adopted in this work (without loss of generality as commented later) for consistency with the CSHELL flutter solver. To set up a linear state-space formulation of Eq. (4), an analytical dependency on k of Q_{hh} is needed. This is generally achieved employing Rational Function Approximation (RFA) strategies. In this work Roger method [18] is used, and the interested reader is referred to [7] for further discussions about different aerodynamic approximations and their impact on robust flutter analysis.

The resulting state-space equation has the following shorthand expression:

$$\begin{bmatrix} \dot{x}_s \\ \dot{x}_a \end{bmatrix} = \begin{bmatrix} \chi_{ss} & \chi_{sa} \\ \chi_{as} & \chi_{aa} \end{bmatrix} \begin{bmatrix} x_s \\ x_a \end{bmatrix} \tag{6}$$

where the vector of aerodynamic states x_a (due to the RFA) and structural states $x_s = [\eta; \dot{\eta}]$ have been introduced, and the state-matrix has been partitioned as:

$$\begin{aligned} \chi_{ss} &= \begin{bmatrix} 0 & I \\ -M^{-1}K & -M^{-1}C \end{bmatrix}; \quad \chi_{as} = \begin{bmatrix} 0 & I \end{bmatrix}; \\ \chi_{sa} &= \begin{bmatrix} 0 & ... & 0 \\ q_\infty M^{-1} A_3 & ... & q_\infty M^{-1} A_{N_Q} \end{bmatrix}; \\ \chi_{aa} &= \begin{bmatrix} -\frac{V}{L_r}\gamma_1 I_{n_s} & 0 & 0 \\ 0 & \ddots & 0 \\ 0 & 0 & -\frac{V}{L_r}\gamma_{N_l-2} I_{n_s} \end{bmatrix}; \end{aligned} \tag{7}$$

with $M = \bar{M}_s - \frac{1}{2}\rho_\infty L_r^2 A_2$, $C = \bar{C}_s - \frac{1}{2}\rho_\infty L_r V A_1$, and $K = \bar{K}_s - \frac{1}{2}\rho_\infty V^2 A_0$ are respectively the aeroelastic inertial, damping, and stiffness matrices, and the matrices A_i with $i = 0, ..., N_Q$ derive from the RFA and are found by applying a linear least-square fitting to Q_{hh} on a selected range of reduced frequencies [18], [7].

III. LFT MODELING EMBEDDED IN THE FSI SOLVER

A. State of practice and current limitations

The LFT modeling of high-order systems is commonly accomplished via numerical approaches. They consist of evaluating the high-fidelity model at scattered values of the parameters in the uncertainty set (and possibly linearizing it, if nonlinear), followed by a model-order reduction to obtain lower-size representations. The family of systems is then interpolated [19] so that a polynomial description is obtained. Finally, algorithms which allow polynomial expressions to be recast into LFTs [12] are applied.

This approach has been applied to aeroelastic systems in the last two decades [20], [8], [9], but some drawbacks can be observed in relation to: accuracy of the LFT; uncertainty descriptions allowed; and computational efficiency. Since it relies on a polynomial interpolation, the accuracy of the numerical LFT depends on the uncertainty set considered. This feature can be exemplified considering Fig. 1, where the subdivision in N stations of a notional wing is depicted. The stations can be interpreted as the areas of the wing where perturbations in the values of the parameters are expected, and thus a better understanding of their influence on flutter is valued. In view of this, it is natural to aim at considering a description characterized by large N (i.e. refined stations' grid) and localized parameters (e.g. a small concentrated mass δ_{M_i} in a wing station).

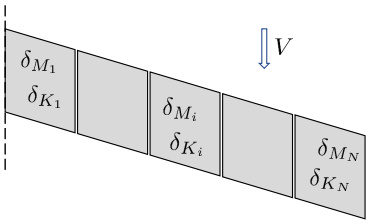

Fig. 1. Schematic uncertainty description of a wing.

An uncertainty description akin to that in Fig. 1 might be challenging when the numerical LFT approach is pursued. The selection of a large number of uncertain parameters as well as of very localized uncertainties (e.g. small nominal values and/or uncertainty ranges) might indeed hamper the effectiveness of the LFT modeling, but also of the μ analysis, algorithms. The ensuing interpolation can indeed: be inaccurate (e.g. small variations in localized uncertainties might not be well captured; or a large number of uncertainties might force to consider a coarse parametric grid); lead to intractable LFTs (due to the Δ-block size); or be computationally intensive (due to the large number of samples to be computed with the FSI solver). This is indirectly confirmed by examples from the literature [9], [20], [8], where a maximum of three parameters were considered, all representing large quantities (e.g. extreme filling levels of the fuel tanks).

Another possible issue was discussed in [20], where it was shown that the simple but widespread (especially for flutter analysis) modal truncation (5) could not be employed as reduction technique because of modal consistency problems among the reduced models. Consistency is highly desirable for the accuracy of the resulting interpolation, thus more sophisticated model reduction strategies were proposed in [8]. As for the computational aspects, note that the numerical LFT approach must be performed anew for any change in the model, and this could be costly depending on the density of the parametric grid.

The aforementioned aspects prompted the research for alternative LFT modeling strategies. In [5] (a foundational contribution to the μ-flutter topic) the uncertainty description is done by introducing a posteriori parametric uncertainties in the generalized structural matrices (5) and in the aerodynamic RFA matrices. This is practical, but the reconciliation between physical source of uncertainties and LFT parameters

is more difficult. A similar approach was taken in [6] for the structural operators, whereas a physical description of the aerodynamic uncertainties directly applied to the GAF matrix was proposed (but limited to frequency-domain (as it is Eq. 4) descriptions).

It is thus considered of interest the development of an alternative LFT formulation which aims at addressing the restrictions and limitations noted above, with particular emphasis on structural parametric uncertainties. For aerodynamic uncertainties alone, the unifying solution from [7] retains already some of the desired features discussed here. Briefly, it allows uncertainties in the original GAF matrix Q_{hh} to be introduced even when a state-space formulation (as it is Eq. 6) is employed for the nominal system by exploiting a particular application of the concept of unmodelled dynamics [4].

B. A symbolic LFT modeling algorithm

The main idea behind the proposed approach is to perform the LFT modeling task at *FSI solver level*. By this, it is meant that the uncertain parameters are introduced in the structural solver when the physical operators are assembled. The main steps entailed by this symbolic modeling algorithm are presented in the flow chart of Fig. 2.

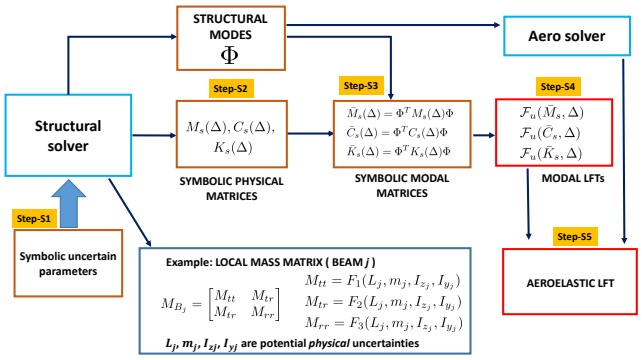

Fig. 2. Symbolic LFT-FSI modeling algorithm's chart.

As an example, let us consider the structural mass matrix M_{B_j} of the beam j:

$$M_{B_j}=\begin{bmatrix} M_{tt} & M_{tr} \\ M_{tr} & M_{rr}\end{bmatrix} \qquad \begin{aligned} M_{tt} &= F_1(L_j,m_j,I_{z_j},I_{y_j}) \\ M_{tr} &= F_2(L_j,m_j,I_{z_j},I_{y_j}) \\ M_{rr} &= F_3(L_j,m_j,I_{z_j},I_{y_j}) \end{aligned} \tag{8}$$

where the subscripts t and r refer to translational and rotational DOFs. The structural parameters L_j, m_j, I_{z_j}, and I_{y_j} are respectively the beam length, mass and moments of inertia, while F_1, F_2, and F_3 are polynomial matrix functions of these properties. When some of these parameters are considered uncertain and thus the functions are not evaluated at the corresponding nominal values, the local physical operator M_{B_j} is a matrix function of the uncertainties. If the parameters are defined as symbolic objects (Step-S1), then $M_{B_j}(\Delta(\delta_{j-\bullet}))$ (where $\bullet = L, m, I_z, I_y$) is a symbolic operator that will contribute to the structural mass matrix M_s (Step-S2). This step is general and can be applied to other contributions to the mass operator (e.g. concentrated masses) and to other operators (e.g. stiffness). Crucially, this setting does not pose in principle any restriction on the number and type of parameters $\delta_{j-\bullet}$ that can be captured (in the example discussed they were generically represented by the structural parameters in (8)).

Once the *symbolic* physical matrices are obtained, a modal truncation is performed (Step-S3):

$$\begin{aligned} \bar{M}_s(\Delta) &= \Phi^T M_s(\Delta)\Phi \\ \bar{C}_s(\Delta) &= \Phi^T C_s(\Delta)\Phi \\ \bar{K}_s(\Delta) &= \Phi^T K_s(\Delta)\Phi \end{aligned} \tag{9}$$

where Δ indicates the uncertainty set gathering the symbolic parameters and the selection of the modal matrix Φ will be discussed in the next subsection. Given the symbolic modal matrices $\bar{M}_s$, $\bar{C}_s$, and $\bar{K}_s$, it is possible to apply standard LFT algorithms [12] which allow polynomial matrices to be recast into the formalism of Eq. (2). In this way, the modal LFTs $\mathcal{F}_u(\bar{M}_s,\Delta)$, $\mathcal{F}_u(\bar{C}_s,\Delta)$, $\mathcal{F}_u(\bar{K}_s,\Delta)$ are obtained (Step-S4). The final step consists in building up the aeroelastic LFT (Step-S5). This can be done by substituting the modal LFTs in the corresponding terms of the state-space model (7), possibly in addition to aerodynamic uncertainties if these are considered (details on Step-S5 can be found in [7], which focused on this task). The size of the aeroelastic LFT can be further reduced in this final stage if simplifications in the occurrence of the uncertainties are made (e.g. by means of the 1-d order reduction technique [12]).

An important feature of the modeling algorithm is that the LFT transformation is applied to the modal operators (Step S3) by exploiting the structure of the aeroelastic equation. This aspect is referred here as *modal-oriented* LFT modeling, to stress the distinction with common numerical approaches where the transformation to LFT is applied directly to the state-matrix [20], [8]. Thanks to this it is possible to build up LFTs where only n_δ structural modes (with $n_\delta \leq n_s$) feature uncertainties. This can be regarded as an extension of what is typically done in nominal flutter analysis, where only the modes with lowest frequencies are retained in the final model. By identifying the minimum number of modes in which uncertainties have to be introduced for an accurate robust flutter analysis, it would then be possible to obtain lower size aeroelastic LFTs for more efficient application of μ. Moreover, the possibility to generate different LFTs, each having a different n_δ, might help to gain understanding in the mechanisms prompting the instability.

A delicate aspect of this formulation is the handling of the modal matrix Φ. First, it should be noted that many of the existing approaches assume for the robust analyses a fixed modal base (typically Φ_0 corresponding to the nominal system) [5], [6], [9]. This is an approximation and potentially a source of error [21] in the predictions since Φ is altered when there are structural uncertainties in Δ, with consequences on both the structural and aerodynamic operators.

Note that, when the operation in Eq. (9) is performed with

a given Φ (e.g. Φ_0) , the obtained symbolic modal matrices are generally full. This is a source of error related to the fixed modal base-assumption, because due to eigenvectors properties, the modal mass and stiffness matrices are actually diagonal. By exploiting the embedding of the LFT modeling in the FSI solver and the adoption of a modal-oriented approach, this inaccuracy can be eliminated a priori by retaining only the diagonal terms (Step S-3 in Fig. 2):

$$\begin{aligned} \bar{M}_s(\Delta) &\equiv diag(\Phi^T M_s(\Delta)\Phi) \\ \bar{C}_s(\Delta) &\equiv diag(\Phi^T C_s(\Delta)\Phi) \\ \bar{K}_s(\Delta) &\equiv diag(\Phi^T K_s(\Delta)\Phi) \end{aligned} \tag{10}$$

While this modification of Step-S3 allows to mitigate the error due to the modes and confine it only to the diagonal terms of the symbolic modal matrices, the fixed modal base assumption can still lead to wrong predictions. To this aim, an iterative algorithm is formulated with the aim to determine (if it exists) a worst-case perturbation $\hat{\Delta}^{cr}$ which makes the system flutter at a user-provided V_μ. The key feature in order to achieve accurate results consists in updating the modal matrix used in Step-S3 with the one corresponding to the perturbation matrix Δ^{cr} computed at the previous iteration step. A similar iterative scheme was proposed also in [21].

The algorithm, see Fig. 3, requires as input the symbolic matrices $M_s(\Delta)$, $C_s(\Delta)$, and $K_s(\Delta)$ from Step-S2, which are held fixed throughout the iterations, and the initial modal base (a standard option is the nominal modal matrix Φ_0). This initialization allows to build the aeroelastic LFT (Step-A1) and μ analysis can thus be performed (Step-A2). The perturbation matrix Δ^{cr} is extracted from the highest peak of the lower bound μ_{LB}, and based on it the associated flutter speed $V_{f\mu}$ can be calculated using the FSI solver (Step-A3). If the difference between $V_{f\mu}$ and the expected perturbed flutter speed V_μ is greater than a given tolerance ϵ_V, the modal base is updated with the matrix Φ^{cr} corresponding to Δ^{cr} (Step-A4) and is used to re-initialize Step-A1. This will entail executing the symbolic LFT algorithm from Step-S3 (Fig. 2) and updating the aerodynamic operator based on Φ^{cr} (recall that perturbations on Φ have an impact on Q_{hh}).

It is stressed the difference between Δ^{cr} and $\hat{\Delta}^{cr}$. The former is provided by the μ-lower bound computation at a generic iteration and, due to the modal base error, might not correspond to a flutter speed $V_{f\mu}$ equal to V_μ. The latter instead determines a flutter speed $V_{f\mu} \approx V_\mu$ within given tolerance and thus is the sought worst-case perturbation.

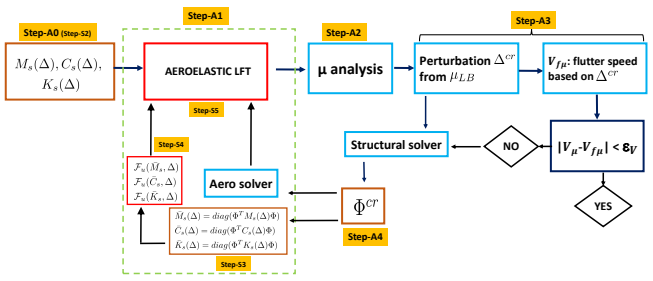

Fig. 3. Iterative scheme block diagram.

To interpret the proposed analysis algorithm from an LFT perspective, let us indicate the aeroelastic LFT available at Step-S5 of the modelling algorithm as:

$$\mathcal{F}_u(M,\Delta) = M_{22}(\Delta)+M_{21}(\Delta)\Delta(I-M_{11}(\Delta)\Delta)^{-1}M_{12}(\Delta) \tag{11}$$

Eq. (11) reflects the fact that it is not possible to express the effect of the uncertainties on $\mathbf{\Phi}$ in the standard linear fractional fashion (2). Crucially, the Δ block affects here also the partitioned matrix M. The iterative scheme proceeds then by updating M with the value of Δ given at the last iteration, that is $\mathcal{F}_u(M,\Delta)$ is approximated as

$$M_{22}(\Delta^{cr}) + M_{21}(\Delta^{cr})\Delta(I - M_{11}(\Delta^{cr})\Delta)^{-1}M_{12}(\Delta^{cr}) \tag{12}$$

where in the first iteration $\Delta^{cr} = 0$ (corresponding to the nominal modal matrix Φ_0) is employed.

IV. Application Example

The modeling and analysis framework proposed in Sec. III is applied to the Joined-wing aircraft configuration known as PrandtlPlane 250 ($PrP250$), a 250 passenger mid-long range aircraft with a Maximum Take Off Weight of 230 tons (see Fig. 4) studied in [10] and other references therein.

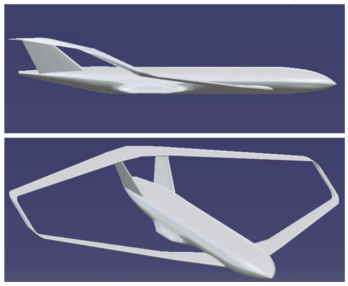

Fig. 4. PrandtlPlane 250-seat concept. See [10].

A. Nominal flutter and uncertainty description

The flutter behaviour of the $PrP250$ configuration without uncertainties is investigated first. The analyses are carried out with CSHELL, and then validated with the commercial software NASTRAN [22], considering only the first 10 structural modes (n_s=10). Results of the flutter analysis are reported in Fig. 5, which shows the imaginary and real parts of the poles of the first five modes as the speed is increased. It is seen on the damping plot (right) that the first mode becomes unstable (indicated in the figure as flutter point) at approximately $V_f = 297\frac{m}{s}$ due to coupling of the first two bending modes before flutter occurs (see coalescence of frequencies in the left plot). It is interesting to add that further studies have considered the effect of an elastic fuselage. Starting from the model in [15], where only its inertial contribution was captured, it has been shown [23] that this additional flexibility in the system highly affects mode III, which is responsible for the onset of flutter at a smaller speed.

Uncertainties in the stiffness and mass parameters are then considered (structural damping was assumed null in

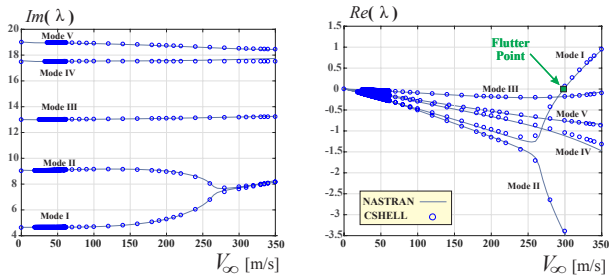

Fig. 5. Nominal flutter analysis of the $PrP250$.

this case study). The FE model has 54 beam elements, and 27 stations are defined by pairing consecutive beams. The stations are shown and numbered on the aircraft right wing sketch given in Fig. 6. In each station the bending stiffness parameter EI_z is considered uncertain, thus the stiffness uncertainty description consists of 27 uncertainties (i.e. $\delta_{EI_{z_j}}$ with j=1,...,27), each allowed to vary within 10% of its nominal value.

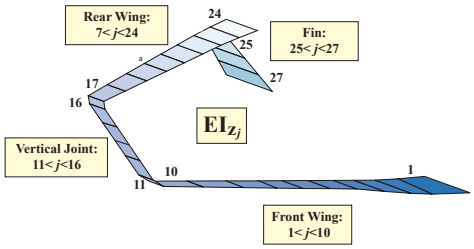

Fig. 6. Stiffness parameters uncertainty description.

As for the mass, the 36 fuel masses m_f gathered in the model, and visualized in Fig. 7, are all assumed uncertain (i.e. $\delta_{m_{f_k}}$ with k=1,...,36) and allowed to vary within 10% of their nominal values.

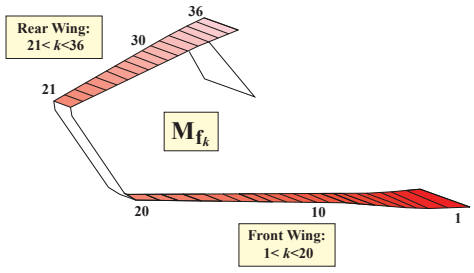

Fig. 7. Mass parameters uncertainty description.

Based on this description, consisting of a total of 63 parameters, the symbolic LFT modeling algorithm is applied. The Δ block of the resulting aeroelastic LFT is:

$$\Delta = \text{diag}(\delta_{EI_{z_1}} I_{10}, ..., \delta_{EI_{z_{27}}} I_{10}, \delta_{m_{f_1}} I_{10}, ..., \delta_{m_{f_{36}}} I_{10}) \quad (13)$$

and consists of 630 real parameters. Despite the adoption of LFT order reduction techniques [12], the size of the LFT is such that it cannot be used for μ calculation at this stage. The very high dimension is a result of: the large number of real parameters captured in the LFT (63), and the presence of uncertainties in all the n_s structural modes (10).

In order to lower the size, firstly a reduced number of parameters is selected based on their contribution to the coefficients of the modal matrices (this can be done in Step-S4 because the modal matrices are available as polynomials in the uncertainties). As a result of this polynomial reduction process, the number of parameters in the LFTs is reduced to 20 for the stiffness and 25 for the mass. Secondly, it is possible to take advantage of the possibility to introduce uncertainties only in a subset of n_δ structural modes. Since the nominal analyses pointed out that flutter is prompted by the coalescence of the first and second bending modes, a small number of modes $n_\delta \leq n_s$ might be sufficient to capture the effect of the uncertainties on flutter. This assumption was confirmed by carrying out analyses for different values of n_δ where a convergence of the predictions for $n_\delta \geq 5$ was observed. Thus, $n_\delta = 5$ is considered and a reduced-order LFT featuring a total size of 225 ($20 \cdot 5$ from the stiffness and $25 \cdot 5$ from the mass) is obtained.

B. Robust flutter analysis

The analysis algorithm in Fig. 3 is finally applied. This will detect a worst-case perturbation $\hat{\Delta}^{cr}$ that makes the aeroelastic system flutter at the selected subcritical speed V_μ. For the present case, $V_\mu = 285\frac{m}{s}$ is chosen considering that from the nominal analysis it holds $V_f = 297\frac{m}{s}$. Fig. 8 shows in the main plot only the upper (μ_{UB}-UB) and lower (μ_{LB}-LB) bounds corresponding to the first iteration (ITER1) of the algorithm, while in the inset the different iterations for the low frequency peak are given. Note that two peaks are clearly observed, a lower frequency one, taking place at approximately ω_1=7.2$\frac{rad}{s}$ and associated to the coalesced modes I-II (responsible for the flutter observed in nominal conditions), and a higher frequency one (at ω_2=13.2$\frac{rad}{s}$). As prescribed by the algorithm, the perturbation matrix extracted from the highest peak of the lower bound is used, and hence the instability related to the 1^{st}-2^{nd} modes flutter will be studied here. This choice is without loss of generality because the same procedure could be applied to another point of the frequency grid by simply carrying out the iterations with respect to the perturbation matrix associated with it.

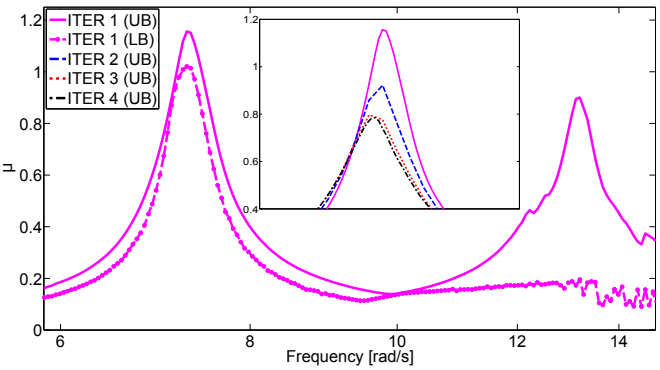

Fig. 8. μ-bounds at different iterations.

In the inset of Fig. 8 the upper bounds at all the other analysis algorithm's iterations (ITER#) are reported. For clarity, the lower bounds are not plotted since the relative gap between bounds for each iteration is similar to the one at ITER1. Tab. I reports the flutter speed $V_{f\mu}$ (calculated by CSHELL) at each iteration and the norm of the critical perturbation matrix. The algorithm achieves in 4 iterations a value of $V_{f\mu}$=285.2$\frac{m}{s}$ which is within 0.15% of the selected V_{μ}=285$\frac{m}{s}$. At each iteration #, the magnitude of $\Delta^{cr}_{ITER\#}$ increases (this was already noticeable from Fig. 8 since smaller μ_{UB} indicates larger norm of the perturbation matrix). Since $\bar{\sigma}(\hat{\Delta}^{cr}) = \bar{\sigma}(\Delta^{cr}_{ITER4}) = 1.47 > 1$, it can be concluded that the joined-wing is guaranteed to be robustly stable at V=285$\frac{m}{s}$ in the face of the allowed modeling uncertainties.

TABLE I

FLUTTER SPEED AND CORRESPONDING PERTURBATION MATRIX'S NORM AT EACH ITERATION.

ITER	$V_{f\mu}\frac{m}{s}$	$\bar{\sigma}(\Delta^{cr})$
1	288.4	0.98
2	287.4	1.23
3	285.9	1.41
4	285.24	1.47

It is also important to consider the frequency content of the information provided by μ, which in this case showed the presence of two distinct peaks. To interpret this, recall that the nominal flutter analyses only detected the presence of the 1^{st}-2^{nd} modes flutter, while it was necessary to augment the model with an elastic fuselage [23] (recall the previous discussion on this point) to find that the higher-frequency mode III would also become critical for flutter. As seen in Fig. 8, robust analysis anticipates this for the present model (which does not include an elastic fuselage) when variations of particular stiffness and mass parameters are allowed in the system. Indeed, the higher frequency peak in the plot occurs at a frequency very close to that of mode III in Fig. 5.

V. CONCLUSIONS

The main contribution of the paper is an integrated LFT modeling and μ analysis strategy to perform robust flutter analysis of high-order uncertainty aeroelastic systems. The main advantages of this formulation are: the uncertainties are defined in the FSI solver and thus have a clear physical meaning; a greater flexibility in the parameters' selection compared to interpolation-based LFTs.

The key idea to achieve this is to perform the LFT modeling step embedded in the FSI solver, leading to an LFT-FSI symbolic approach. A possible issue is that the dependence of the modal matrix on the uncertainties is not captured explicitly, and thus an iterative analysis algorithm, which updates the matrix based on the perturbation matrix predicted by μ, is proposed. Given a nominally stable speed, this framework provides a worst-case perturbation matrix provoking the loss of stability in the perturbed system, and thus allows robustness of the system in the operational range of the aircraft to be established. Application to an unconventional aircraft configuration showcases the potential of the framework and points out its capability to predict instability mechanisms not detected with nominal analyses.

REFERENCES

[1] W. P. Rodden, *Theoretical and Computational Aeroelasticity*. Crest Publishing, 2011.

[2] C. Pettit, "Uncertainty Quantification in Aeroelasticity: Recent Results and Research Challenges," *Journal of Aircraft*, vol. 41, no. 5, pp. 1217–1229, 2004.

[3] B. P. Danowsky, J. R. Chrstos, D. H. Klyde, C. Farhat, and M. Brenner, "Evaluation of Aeroelastic Uncertainty Analysis Methods," *Journal of Aircraft*, vol. 47, no. 4, pp. 1266–1273, 2010.

[4] K. Zhou, J. C. Doyle, and K. Glover, *Robust and Optimal Control*. Prentice-Hall, Inc., 1996.

[5] Lind, R. and Brenner, M., *Robust Aeroservoelastic Stability Analysis*, ser. Advances in Industrial Control. Springer, 2012.

[6] D. Borglund, "The μ-k Method for Robust Flutter Solutions," *Journal of Aircraft*, vol. 41, no. 5, pp. 1209–1216, 2004.

[7] A. Iannelli, A. Marcos, and M. Lowenberg, "Aeroelastic modeling and stability analysis: A robust approach to the flutter problem," *International Journal of Robust and Nonlinear Control*, vol. 28, no. 1, pp. 342–364, 2018.

[8] C. Poussot-Vassal and C. Roos, "Generation of a reduced-order LPV/LFT model from a set of large-scale MIMO LTI flexible aircraft models," *Control Engineering Practice*, vol. 20, no. 9, pp. 919–930, 2012.

[9] S. Bennani, B. Beuker, J. van Staveren, and J. Meijer, "Flutter Analysis for the F-16A/B in Heavy Store Configuration," *Journal of Aircraft*, vol. 42, no. 6, pp. 1566–1575, 2005.

[10] A. Frediani, V. Cipolla, and E. Rizzo, "The PrandtlPlane configuration: Overview on possible applications to civil aviation," in *Variational Analysis and Aerospace Engineering: Mathematical Challenges for Aerospace Design*. Springer US, 2012, vol. 66, pp. 179–210.

[11] R. Cavallaro and L. Demasi, "Challenges, ideas, and innovations of joined-wing configurations: A concept from the past, an opportunity for the future," *Progress in Aerospace Sciences*, vol. 87, pp. 1 – 93, 2016.

[12] J. Magni, "Linear fractional representation toolbox modelling, order reduction, gain scheduling," DCSD, ONERA, Systems Control and Flight Dynamics Department," Technical Report TR 6/08162, 2004.

[13] G. Balas, R. Chiang, A. Packard, and M. Safonov, *Robust Control Toolbox*, 2009.

[14] L. Demasi and E. Livne, "Dynamic Aeroelasticity of Structurally Nonlinear Configurations Using Linear Modally Reduced Aerodynamic Generalized Forces," *AIAA Journal*, vol. 47, pp. 71–90, 2009.

[15] R. Cavallaro, R. Bombardieri, L. Demasi, and A. Iannelli, "Prandtlplane Joined Wing: Body freedom flutter, limit cycle oscillation and freeplay studies," *Journal of Fluids and Structures*, vol. 59, pp. 57–84, November 2015.

[16] E. Albano and W. Rodden, "A doublet lattice method for calculating lift distributions on oscillating surfaces in subsonic flows," *AIAA Journal*, vol. 7, no. 2, pp. 279–285, 1969.

[17] T. Belytschko, W. Liu, and B. Moran, *Nonlinear finite elements for continua and structures*. Wiley, 2000.

[18] K. Roger, "Airplane math modeling methods for active control design," *AGARD-CP-228*, August 1977.

[19] C. Roos, G. Hardier, and J.-M. Biannic, "Polynomial and rational approximation with the APRICOT library of the SMAC toolbox." Proceedings of the IEEE Multiconference on Systems and Control, October 2014.

[20] J. Torralba, F. Demourant, G. Puyou, and G. Ferreres, "A Method for Flexible Aircraft LFT Modelling." IEEE European Control Conference, 2009.

[21] S. Heinze and D. Borglund, "Robust Flutter Analysis Considering Mode Shape Variations," *Journal of Aircraft*, vol. 45, no. 3, pp. 1070–1074, 2008.

[22] W. P. Rodden and E. H. Johnson, *User Guide V 68 MSC/NASTRAN Aeroelastic Analysis*. MacNeal-Schwendler Corporation, 1994.

[23] A. Iannelli, "Robust linear and nonlinear modelling and analysis approaches for uncertain aeroelastic systems," Ph.D. dissertation, University of Bristol, 2019.